Ropivacaine Induce G0 / G1 Phase Cell Cycle Arrest and Apoptosis of PC12 Cells Via Inhibiting Mitochondrial STAT3 Translocation

Lian Zeng
Hubei University of Medicine
Zhen Zhang
Hubei University of Medicine
Fuyu Zhang
Hubei University of Medicine
Chenguang Liu
Hubei University of Medicine
Jiafeng He
Hubei University of Medicine
Huaxian Chen
Hubei University of Medicine
Qingsong Wang
Hubei University of Medicine
Xudong Ding
Hubei University of Medicine
Huiyu Luo (603983267@qq.com)
Hubei University of Medicine https://orcid.org/0000-0003-2126-223X

Research article

Keywords: ropivacaine, neurotoxicity, STAT3, mitoSTAT3, PC12 cells, spinal cord

Posted Date: February 22nd, 2021

DOI: https://doi.org/10.21203/rs.3.rs-216194/v1

Version of Record: A version of this preprint was published at Inflammation on August 20th, 2021. See the published version at https://doi.org/10.1007/s10753-021-01508-w.

Abstract

Signal transducer and activator of transcription 3 (STAT3) has been shown to have neuroprotective effects via the non-canonical activation and mitochondrial translocation, but its effect on ropivacaine induced neurotoxicity is unclear. Our previous studies have revealed that apoptosis was an important mechanism of ropivacaine induced neurotoxicity, so this study is to explore the relationship between STAT3 with ropivacaine induced apoptosis. Our results showed that ropivacaine decreased PC12 cell viability, arrested the cells in the G0 / G1 phase, induced cell apoptosis and oxidative stress, and damaged mitochondrial functions. In addition, the serine727 (Ser727) phosphate activation of STAT3 was inhibited by ropivacaine. Ropivacaine decreased the p-STAT3 (Ser727) expression in the mitochondria, and increased p-STAT3 (Ser727) expression in the cytoplasm, so that it inhibited mitochondrial STAT3 translocation. To explore the potential connection between STAT3 with ropivacaine, the autodock-vina was used to examine the interaction between STAT3 and ropivacaine, and results showed that ropivacaine could bind to STAT3. Furthermore, the apoptosis of the spinal cord was increased and the p-STAT3 (Ser727) expression in the spinal cord was reduced after ropivacaine treatment. our findings illustrated that ropivacaine induced neurotoxicity by increasing the apoptotic levels, the activation and mitochondrial translocation of STAT3 were inhibited by ropivacaine. There may be an internal connection between these phenomena.

Introduction

Ropivacaine, as an amide local anesthetic, has been widely used in clinical practice. Because of the long-lasting and stable anesthetic effects, ropivacaine is mainly used for pain management and regional anesthesia, which has the characteristic of sensorimotor separation (Martin-Flores M, 2019). However, some studies have shown that ropivacaine has cytotoxicity(Cai XY et al., 2015;CM C et al., 2012), including muscle toxicity, neurotoxicity, and cardiotoxicity. In recent years, increasing attention has been paid to the neurotoxicity because it is directly related to the recovery of patients after surgery(Aps J and Badr N, 2020), but the mechanism of ropivacaine induced neurotoxicity is unclear. In past decades, a growing body of evidence has revealed that apoptosis plays an important role in the ropivacaine induced neurotoxicity (Chen Y et al., 2019;Wang S et al., 2019;Wen X et al., 2019), most studies have demonstrated that ropivacaine may induce neurotoxicity via activating apoptosis and up-regulating apoptosis-related genes. These were consistent with our previous findings that ropivacaine could induce apoptosis of PC12 cells which was related to the activation of the Fas / Fasl signaling pathway (Zeng Y et al., 2019).

The signal transducer and activator of transcription 3 (STAT3), as a transcriptional enhancer of acute-phase genes activated by IL-6 (Sgrignani J et al., 2018), had been demonstrated to be involved in many biological activities including apoptosis, cell cycle progression, cell migration and angiogenesis (Guanizo AC et al., 2018;Hillmer EJ et al., 2016;Vogel TP et al., 2015). Most studies have indicated that STAT3 can inhibit the cell apoptosis, depending on the mitochondrial STAT3 translocation (Fathi N et al., 2018;Srivastava J and DiGiovanni J, 2016). As we know, the transduction of downstream signals initiated

by STAT3 depends on the phosphorylation of specific amino acids, the most representative of which is the tyrosine705 (Tyr705) or serine727 (Ser727) phosphorylation(Sgrignani J,Garofalo M,Matkovic M,Merulla J,Catapano CV and Cavalli A, 2018). The Ser727 phosphorylation of STAT3 can induce STAT3 to translocate in the mitochondrial (mitoSTAT3), which executes transcription-independent functions(Srivastava J and DiGiovanni J, 2016). The mitoSTAT3 have an effect of anti-apoptosis, mainly through improving damaged mitochondrial functions include regulating the mitochondrial electron transport chain (ETC) activities and increasing the mitochondrial electron transport chain (MMP) to elevate ATP production(Yang R and Rincon M, 2016). MitoSTAT3 has been reported to produce a protective effect of many diseases include ischemia (Heusch G et al., 2011;Szczepanek K et al., 2011), immune system disease (Flanagan SE et al., 2014), and so on (Steward-Tharp SM et al., 2014). To date, no study has been conducted to investigate the role of mitoSTAT3 in ropivacaine induced neurotoxicity.

In the present study, our results showed that ropivacaine could not only inhibit STAT3 phosphorylation and activation but also decrease the translocation of mitoSTAT3, which might contribute to ropivacaine induced neurotoxicity in PC12 cells and the spinal cord. Further investigation confirmed that ropivacaine could arrest the cell cycle, increase apoptosis, damage mitochondrial function, and induce oxidative stress, which were related to the inhibition of STAT3 translocation.

Materials And Methods

Rat pheochromocytoma cell line (PC12) was purchased from the Cell Bank of Shanghai Institute of Chinese Academy of Sciences. These cells were maintained in the Dulbecco's modified Eagle's medium (DMEM) with 10% fetal bovine serum (FBS) and 1% penicillin/streptomycin. The cell counting kit-8 (CCK-8) from Biosharp (Shanghai, China), lactate dehydrogenase (LDH), superoxide dismutase (SOD), and malondialdehyde (MDA) test kits from wanleibio (Shenyang, China), reactive oxygen species (ROS), Mitochondrial membrane potential test kits (JC-1) and Mitochondrial protein extraction kits purchased from KeyGEN BioTECH (Jiangsu, China), primary antibodies against CyclinE1, CDK4, p21, Bax, Bcl-2 from Proteintech (Wuhan, China), Caspase-3, STAT3, p-STAT3, and COXIV from Wanleibio (Shenyang, China) were used in the present study.

Cell cultured and drug administration

PC12 cells were grown in environment containing 10% CO^2 at 37°C. When the cells confluence 70–80%, 0.25% trypsin with EDTA was used to digest the cells which were then harvested after centrifugation. These cells were divided into the control group, and different ropivacaine groups (0.5mM, 1 mM, 2 mM). After incubation with serum-free high-glucose DMEM for 12 h, ropivacaine (Hengrui medicine, Jiangsu, China) was added to the medium followed by incubation for 24 h.

Cell viability detection

PC12 cells were seeded in a 96-well plate at a density of 5×10^3 cells/well and then treated with PBS or various concentrations of ropivacaine (0.5 mM, 1 mM, 2 mM, 4 mM, 8 mM) in 100 μl of medium for the

indicated times. There were six wells in each group. After incubation for 24 h, 10 μl of CCK-8 solution was added to each well, followed by incubation for 2 h at 37°C. The absorbance was measured in a microplate reader (Biotek, Winooski, VT, USA) at a wavelength of 450 nm.

ROS, SOD, MDA, and LDH determination

The cells and cell supernatant were collected to measure the levels of SOD, MDA and LDH with corresponding kits according to the manufactures' instructions. Then, PC12 cells were seeded in a 12-well plate at a density of 5×10^4 cells/well. After treatment with different concentrations of ropivacaine, cells were incubated with dihydroethidine (DHE) for 60 min in dark following the instructions of ROS assay kit. Subsequently, the fluoresce intensity was observed under a fluorescence microscope (Olympus, Japan) and the average optical density was measured by ImageJ software.

Mitochondrial and nuclear DNA ratio (mtDNA / nDNA)

The DNAzol™ Reagent (Invitrogen™, USA) was used to extracted the genomic DNA according to the manufacturer's instructions. DNA was quantified with NanoPhotometer (Implen, Germany). The ratio of mtDNA / nDNA was measured by real-time PCR. The amplification of mitochondrial cytochrome c oxidase subunit II (COII, mitochondrial-encoded gene) and β-actin (nuclear-encoded gene) was done with Real-time PCR. The primer used were as follows: COII: 5'-TGAGCCATCCCTTCACTAGG-3'(sense) and 5'-TGAGCCGCAAATTTCA GAG-3' (anti-sense);β-actin: 5'-CTGCTCTTTCCCAGATGAGG-3'(sense) and 5-CCACAGCA CTGTAGGGGTTT-3' (anti-sense).

Mitochondrial staining

PC12 cells were seeded in a 12-well plate at a density of 1×10^4 cells/well after treated with different concentrations of ropivacaine for 24 h. Then, cells were incubated with Mito-Tracker Red CMXRos (Beyotime, Shanghai, China) according to the instructions. Subsequently, cells were fixed in 4% PFA, and Hochest33258 was used to label the nuclei. Finally, the fluoresce intensity was observed under a fluorescence microscope and the average optical density was measured by ImageJ software.

Mitochondrial membrane potential assay

Mitochondrial membrane potential (MMP) assay was based on JC-1 staining (5,5',6,6'-tetrachloro-1,1'3,3'-tetraethylbenzimidazolcarbocyanine iodide). JC-1 has two forms including monomers and polymers, the emission spectra of which are different. When the mitochondrial membrane potential reduces, the JC-1 polymer with red fluorescence decreases, and so JC-1 monomer with green fluorescence was in the cytoplasm. Following the instructions of JC-1 assay kits, the flow cytometry and fluorescence microscopy were done to measure MMP and the average optical density was determined by ImageJ software.

Mitochondrial separation, extraction of mitochondrial proteins

Mitochondria separation was based on the differential centrifugation. According to the manufacturer's instructions, the cells were broken down by the Ultrasonic Crusher (Sonic, USA). Then, the cell debris and

large organelles were removed by low-speed differential centrifugation (800 ·g). Finally, the mitochondria were harvested by high-speed differential centrifugation (15000 ·g). The extraction of mitochondrial proteins was done after lysing mitochondria with lysis buffer containing a protease inhibitor and a phosphatase inhibitor. The mitochondrial proteins were used for Western Blot.

Quantitative real-time PCR

PC12 cells were digested with trypsin and seeded into 6-well plates cultured for 2 days. Then, cells were treated with different concentrations of ropivacaine for 24h. Total RNA was extracted with Trizol reagent (Invitrogen, USA), and the concentrations were measured by NanoPhotometer (Implen, Germany). A total of 1μg RNA was reversely transcribed into cDNA according to the instructions of RT reagent kit (Promega, USA). SYBR-based real-time PCR experiments were done to detect the mRNA expression of Bax, Bcl-2, Caspase-3, p53, p21, CDK-4, and CyclinE1 using an ABI 7500 platform. The $2^{-\Delta\Delta CT}$ method was used to analyze the data. The primers were used as follow Bax 5'-CTGAGCTGACCTTGGAGC – 3' (forward), 5'-GACTCCAGCCACA AAGATG-3'(reverse) Bcl-2 5'-ATGCCAAGGGGGAAACAC-3' (forward), 5'-CACGGCCGAAAGAGAGA A-3'(reverse) Caspase-3 5'-GAAAGCCGAAACTCTTCATCA-3' (forward), 5'-ATAGTAACCG GGTGCGGTAG-3'(reverse), p53 5'-GCTGAGTATCTGGACGACAGG-3(forward), 5'-AGCGT GATGATGGTAAGGATG-3' (reverse), p21 5'-CTCTGAAGATGTGCCTATGG-3' (forward) 5'-CGAATTTCTCGGACTAATGT-3' (reverse), CDK-4 5'-ACCAGGACCTACGGACATAC-3' (forward) 5'-TACAGCCAACACTCCACATA-3' (reverse) CyclinE11 5'-TGATGATTCAGCG TGCGTGGAC-3' (forward) 5'-CAAGACGGGAAGTGGGGAGG-3' (reverse), GAPDH, 5'-GGCTACACTGAGGACCAGGTT-3' (forward) 5'-TGCTGTAGCCATATTCATTGTC-3'(reverse).

Western Blot

The PC12 cells were lysed with pre-cold RIPA lysis buffer. After centrifugation (12,000 rpm/min) for 15 min at 4℃, the protein concentration was measured with a bicinchoninic acid (BCA) protein assay kit (Beyotime, Shanghai, China). A total of 40 μg proteins were subjected to protein separation by the sodium dodecyl sulfate-polyacrylamide gel electrophoresis (SDS-PAGE). Proteins were then transferred to a polyvinylidene fluoride (PVDF) membrane. The membranes were incubated with 5% non-fat skim milk for 1 h. The membranes were incubated with primary antibodies (Bax, 1:1000; Bcl-2, 1:1000; Caspase3, 1:1000; STAT3, 1:1000; p-STAT3 (Ser727), 1:1000; COXIV: 1:1000) at 4℃ overnight, and then with HRP-linked secondary antibody for 1 h at room temperature. Specific proteins were detected by enhanced chemiluminescence assay (Bio-rad, USA), and the protein bands were quantified with Image Lab software (Bio-rad, USA).

Detection of cell cycle and apoptosis by flow cytometry

PC12 cells were seeded in a 6-well plate at a density of 1×10^6 cells/well after treated with different concentrations of ropivacaine for 24 h, cells were collected and centrifuged at 1000 rpm/min for 5 min at 4°C. After washing with PBS, the cell pellet was fixed in 500 μL of 70% cold ethanol for at 2 h. Before flow cytometry, the cells were washed with PBS, and incubated with 100 μL of RNase. The resulting suspension was incubated at 37°C for 30 min. Subsequently, 400 μL propidium iodide was added for

nuclear staining at 4°C in dark for 30 min. Cell cycles were analyzed using flow cytometry (BD, San Jose, CA). The apoptosis was detected as follows. PC12 cells in each group were digested with trypsin. Then, cells were centrifuged at 1000 rpm/min for 10 min, and the supernatant was removed. The cells were washed twice with PBS and centrifuged to remove the supernatant. 500 μl of buffer solution was added to cell suspension. Then, 5 μL of Annexin V and 10 μL of propidium iodide was added, followed by incubation at room temperature for 30 min in dark, apoptosis was detected by flow cytometry and apoptosis rate was calculated.

Immunofluorescence staining

The cells mitochondria were labeled by Mito-Tracker Red CMXRos according to the manufacturer's instructions. Cells were fixed in 4% PFA and permeabilized with 0.2% Tween X-100. After being blocked with normal goat serum, cells were incubated with rabbit anti-rat p-STAT3 (1:200) overnight at 4℃, and the second antibody (1:1000) was incubated for 1 h at 37℃ in dark. Hochest33258 was added followed by incubation for 5 min to label nuclei. The fluorescence microscope (Olympus, Japan) was used to observe the cells. The fluorescence intensity was analyzed with ImageJ software.

Molecular docking

Structure-based virtual screening was employed with molecular docking program Autodock Vina (version 1.1.2). The PyMol (version 2.3) was used to generate the 3D schematic representation of STAT3 protein (PDB ID: 6QHD) which was extracted by in The Research Collaboratory for Structural Bioinformatics Protein Data Bank database. The 2D schematic representation of the interaction between ligand and other amino acid residues was shown by LigPlus (version 2.1). In order to detect whether ropivacaine competitively bind the STAT3 peptide, the ropivacaine molecular structure (PubChem CID: 175804) was obtained from PubChem database. The ligand and the receptor pdb were converted to pdbqt file by AutoDock Tools following the autodock vina tutorial, and the grid size in XYZ was set at 96,66,118, which is large enough to cover all potential pockets in the STAT3 monomer.

Animals and treatment

All procedures performed in studies involving animals were in accordance with the ethical standards of animal ethics committee of Hubei University of Medicine ((IACUC number: 2018DW003), Eight-week-old Sprague Dawley (SD) rats, weighing 200-300g, were purchased from the Experimental Animal Center of Hubei University of Medicine (Hubei, China). The rats were given access to food and water and housed in an environment with relative humidity of 50–60% and 12/12h light/dark cycle for 1 week before surgery. Rats were anesthetized with 10% chloral hydrate (300 mg/kg body weight, Beyotime Biotechnology, Shanghai, China). The animal was established as a previous reported (Y H et al., 2016). A PE-10 catheter was inserted through the L4 / L5 intervertebral space (depth 2 cm) to the L1-L2. The cannulated rats observed for five days and rats with the neurological injury were not included for further experiment. The remaining rats were randomly divided into four groups (n = 5 per group), including control group (saline group), 0.5% ropivacaine group (0.5% Rop), 1% ropivacaine group (1% Rop) and 2% ropivacaine group

(2% Rop). All rats were received 8 injections at 1.5 h intervals for 12h. After injection, rats were observed for 48 h and those with movement disorders were removed from this study.

TUNNEL staining and Immunohistochemistry

The fresh spinal cord tissues were fixed in 4% PFA. After being embedded with paraffin, the paraffin blocks were cut into 3 mm slices. Then, they were detected with TUNNEL staining according to the manufacturer's instruction to detect the apoptosis in the spinal cord. The protein expression of p-STAT3 (Ser727) in the spinal cord was detected by Immunohistochemistry.

Statistical analysis

Statistical analysis was performed using SPSS version 22.0 software. The quantitative data were expressed as mean ± standard deviation (SD). The comparisons between two groups was done with Student's t-test. The comparison among groups were performed by one-way ANOVA. A value of $P < 0.05$ was considered statistically different.

Results

Ropivacaine decreased viability and reduced the protrusions numbers in PC12 cells

To determine the effects of ropivacaine on PC12 cell viability, CCK-8 assay was done in these cells after treatment with different ropivacaine concentrations (0.5 mM, 1 mM, 2 mM, 4 mM, 8 mM) for 24 h. As shown in Fig. 1A, compared with the control group, ropivacaine suppressed PC12 cell viability in a dose-dependent manner. The half lethal concentration of ropivacaine was 3.24 mM. As we know, PC12 cells are a neuron-like cell line, they have long fusiform with protrusions, but after treatment with ropivacaine, the protrusions reduced, and the cells became round, which represented the loss of the neuronal characteristics. Those results indicate that ropivacaine exerted significant toxic effects on the PC12 cells by inhibiting cell viability.

Ropivacaine arrested PC12 cells in the G0/G1 phase

To explore the effect of ropivacaine on cell death pathway, the cell cycle was detected by flow cytometry in ropivacaine-treated PC12 cells. As shown in Fig. 2A, exposure to different concentrations of ropivacaine for 24 h significantly increased the number of cell in the G0/G1 phase and decreased the number of cell in the G2/M phase as compared to the control group, but ropivacaine had no influence on the S phase. In addition, the expression of genes that regulate the cell cycle of p21, CyclinE1 and CDK4 was detected. After ropivacaine treatment, the mRNA and protein expressions of p21 increased, but the mRNA and protein expression of CyclinE1 and CD4 were inhibited, which indicates that ropivacaine induced PC12 cell death via arresting the cell cycle (Fig. 2C, 2D, 2E).

Ropivacaine induced the apoptosis of PC12 cells and the spinal cord

To determine the effect of ropivacaine on the apoptosis of PC12 cells and the spinal cord, the flow cytometry was used to detected the apoptosis rate of PC12 cells, the results were consistent with our previous study, ropivacaine increased apoptosis in a dose-dependent manner (Fig. 3D). In addition, the mRNA and protein expression of apoptosis-related genes included Bax, Bcl-2 and Caspase 3 were also detected, as shown in Fig. 3A, ropivacaine up-regulated the expression of pro-apoptotic genes and down-regulated the anti-apoptotic gene at mRNA and protein levels. To further explore the effect of ropivacaine on the spinal cord, a rat model was established with a subarachnoid catheter. After the treatment with ropivacaine at different concentrations, TUNNEL staining was to detect the apoptosis of the spinal cord. Compared to the control group, ropivacaine increased the apoptosis rate in the spinal cord in a dose-dependent manner (Fig. 3E, 3F).

Ropivacaine induced oxidative stress in PC12 cells

The oxidative stress was assessed in PC12 cells after ropivacaine treatment by measuring SOD, MDA, ROC, and LDH. As shown in Fig. 2A, compared with the control group, 1 mM ropivacaine significantly increased ROS in the cytoplasm. After treatment with different ropivacaine concentrations of ropivacaine (0.5 mM, 1 mM, and 2mM), ropivacaine increased the MDA, and LDH increased and suppressed the SOD reduced in a dose-dependent manner. These results suggest ropivacaine induces the oxidative stress damage in the PC12 cells.

Ropivacaine induced mitochondrial dysfunction in PC12 cells

To assess the impact of ropivacaine on mitochondria of PC12 cells, a JC-1 test kit was used to detect the MMP of PC12 cells, and the flow cytometry and fluorescence microscopy were done to assess the mitochondrial function. As shown in Fig. 5A, compared with the control group, ropivacaine reduced the amounts of JC-1 polymer in a dose-dependent manner, which indicates the reduction of MMP in PC12 cells after ropivacaine treatment. As shown in Fig. 5B, in the control group, cells had with strong red and green fluorescence, but in the 1 mM ropivacaine group, the MMP decreased, and cells had strong green fluorescence but low red fluorescence. In addition, Mito-Tracker Red CMXRos was used to label mitochondrial with normal function. As shown in Fig. 5D, compared with the control group, 1 mM ropivacaine significantly reduced the number of mitochondria with normal function in PC12 cells, the mtDNA / nDNA ratio kit was determined to assess the amounts of mitochondria. The result showed treatment with ropivacaine reduced the mtDNA / nDNA ratio in a dose-dependent manner (Fig. 5F). Those results demonstrate that ropivacaine causes mitochondrial dysfunction in PC12 cells.

Ropivacaine inhibited STAT3 activation and mitoSTAT3 translocation

To investigate the effect of ropivacaine on the STAT3 signaling pathway in PC12 cells and the spinal cord, STAT3 phosphorylation and upstream transduction proteins expression were evaluated using Western Blot, and the distribution of phosphorylated STAT3 in subcellular compartments was assessed by Western Blot and Immunofluorescence staining, As shown in Fig. 6A, ropivacaine inhibited the serine727 residue phosphorylation of STAT3 and down-regulated IL-6 expression in PC12 cells. In addition, ropivacaine decreased p-STAT3 (ser727) expression in mitochondrial fraction, but increased it in the cytoplasmic fraction (Fig. 6B). Which indicated that ropivacaine inhibited the mitochondrial STAT3 translocation. The result of Immunofluorescence was consistent with Western Blot, ropivacaine reduced the co-localization between p-STAT3 (ser727) with mitochondria in a dose-dependent manner (Fig. 6D). To further explore the effect of ropivacaine on p-STAT3 (ser727) expression in the spinal cord, as expected, ropivacaine inhibited the p-STAT3 (Ser727) expression of the spinal cord in a dose-dependent manner (Fig. 6E). Finally, to explore the potential relationship between STAT3 and ropivacaine, Autodock-Vina was to verify the interaction between them. As shown in Fig. 6F, the pocket was composed of Asn257, Ala377, Glu324, Ile258, Gln326, Pro333, Pro336, Asp 334, Ala250, Cys251 and Pro256. They interacted through hydrophobic bond to affect the activation of STAT3, and further confirming the inhibitory effect of ropivacaine on STAT3 activation.

Discussion

Ropivacaine, as a representative of the long-acting local anesthetics (LAs), is available for the spinal anesthesia, and its duration is 1.6-6 h (Z S et al., 2012). However, some clinical studies have shown that ropivacaine may induce severe neurotoxic side effects after intravenous injection in recent years. Some experiments have also demonstrated that ropivacaine induces neurotoxicity after the long-term exposure to ropivacaine at a high-concentration (A B et al., 2017;S C and S S, 2018;W Z and BM G, 2008). Since Yamashita et al. first reported the neurotoxicity of ropivacaine (Yamashita A et al., 2003), many studies have been conducted to explore and compare the neurotoxicity of LAs commonly used in the clinical practice, including lidocaine, and bupivacaine (Byram SC et al., 2020;Lirk P et al., 2008). Although it had been reported that ropivacaine has the least neurotoxicity among the LAs tested, increasing attention has been paid to the safety of ropivacaine (Yamashita A,Matsumoto M,Matsumoto S,Itoh M,Kawai K and Sakabe T, 2003). Currently, the clinical dosage of ropivacaine is still controversial. It has been reported that injection of high-dose ropivacaine into the epidural space or subarachnoid space can shorten the onset time and increases the motor block effect (Guryay D et al., 2008), while other studies have shown the increased risk of neurotoxicity after exposure to a high-dose ropivacaine (Takenami T et al., 2002). Hence, it is important to investigate the mechanism underlying the ropivacaine induced neurotoxicity, which is helpful for the development of preventive measures and will make the spinal anesthesia safer.

The mechanism of ropivacaine induced neurotoxicity is unclear, and some studies reported it is related to cell apoptosis. Our previous study also revealed that ropivacaine increased apoptosis via up-regulating Fas / Fasl expression in PC12 cells (Zeng Y,Wang R,Bian Y,Chen W and Peng L, 2019), which were also confirmed by Wang et al. (S W et al., 2019). As we know, apoptosis may execute in two pathways: the death receptor pathway and the mitochondrial pathway (Zeng Y,Wang R,Bian Y,Chen W and Peng L,

2019). The death receptor pathway is represented by the up-regulation of Fas/Fasl expression, and the mitochondrial pathway is characterized by the mitochondrial dysfunction. In addition to inducing neurotoxicity through the death receptor pathway, ropivacaine has also been proved to cause neuronal damage by impairing the mitochondrial function. Niu et al. reported ropivacaine affected the mitochondrial biogenesis of neuronal cells by reducing the mitochondrial mass and impairing the mitochondrial respiratory rate via suppressing PCG-1a (Z N et al., 2018). In the present study, our findings confirmed that apoptosis played an important role in the ropivacaine induced neurotoxicity. At first, the cell viability was detected after treatment with different concentrations of ropivacaine. Results showed that ropivacaine decreased the cell viability in a dose-dependent manner. In addition, ropivacaine reduced the protrusions of PC12 cells and cells became round after ropivacaine treatment, which means the cell death increases. In order to determine the cell death pathway induced by ropivacaine, we analyzed the change of cell cycle and apoptosis of ropivacaine-treated PC12 cells using flow cytometry, and results showed that ropivacaine arrested the PC12 cells in G0/G1 phase and increased cell apoptosis. The mRNA and protein expressions of genes regulating the cell cycle and apoptosis were further detected in cells after ropivacaine treatment. p21 is one of those genes that block the cell cycle progression (El-Deiry WS, 2016), and p21 expression increased in the PC12 cells with an increase of ropivacaine concentration. On the contrary, CyclinE1 and CDK4 are the key genes for the maintenance of normal cell cycle progression (Lim S and Kaldis P, 2013;Schade AE et al., 2019;Xu W and McArthur G, 2016). Our results showed that the expression of CyclinE1 and CDK4 in PC12 cells significantly reduced after ropivacaine treatment. Bax and Caspase 3 are the pro-apoptotic proteins in the mitochondrial pathway, and BCL-2 is an anti-apoptotic protein. Our results showed ropivacaine increase the expression of Bax and Caspase 3 in the PC12 cells and inhibit the expression of Bcl-2, which suggests that the mitochondrial apoptosis pathway is involved in the ropivacaine induced neurotoxicity.

To further clarify the effects of ropivacaine on the cellular oxidative stress and mitochondria, the reactive oxygen species (ROS) generation was assessed in cells before and after ropivacaine treatment. Our results showed that the ROS increased with the increase in the concentration of ropivacaine. Similarly, the contents of MDA and LDH also increased significantly, while the level of SOD decreased after ropivacaine treatment. These suggest ropivacaine induces cellular oxidative stress in PC12 cells. Those results were consistent with those reported by Chen et al (Chen Y,Yan L,Zhang Y and Yang X, 2019). Next, the mitochondria function was examined in PC12 cells treated with ropivacaine. Our results confirmed that ropivacaine induced cell mitochondrial dysfunction, which was mainly manifested the decreased of MMP and the ratio of mtDNA / nDNA. Those results were also confirmed by other studies (Y C et al., 2019;Z N,J T,Y R and W F, 2018).

On the basis above findings, we further investigated the role of STAT3 in the ropivacaine induced apoptosis. STAT3 was first described as a transcriptional enhancer of acute-phase genes activated by IL-6, which mediated extracellular signals such as cytokines and growth factors through interacting with polypeptide receptors on the cell surface(You L et al., 2015). The canonical STAT3 signaling becomes transcriptionally activated primarily by tyrosine phosphorylation (Tyr705). Activated STAT3 translocate to the nucleus, and binds to sequence-specific DNA elements for consequent transcription of target

genes(Cui P et al., 2020). The canonical STAT3 pathway has been demonstrated to promote tumor development(Fathi N,Rashidi G,Khodadadi A,Shahi S and Sharifi S, 2018). The non-canonical STAT3 signaling is represented by serine phosphorylation (Ser727), and STAT3 phosphorylated at Ser727 functions to rescue the impaired mitochondrial function after exposure to the stimuli(Srivastava J and DiGiovanni J, 2016). When apoptosis is induced via the mitochondrial pathway, the non-canonical STAT3 signaling is activated to further protect cells against apoptosis. Except for the non-canonical pathway, STAT3 has been shown to regulate the mitochondrial function by transporting to the mitochondria (mitoSTAT3), which is also dependent on serine phosphorylation (Ser727) (Szczepanek K,Chen Q,Derecka M,Salloum FN,Zhang Q,Szelag M,Cichy J,Kukreja RC,Dulak J,Lesnefsky EJ and Larner AC, 2011;Yang R and Rincon M, 2016). As expected, ropivacaine inhibited the activation of STAT3 by down-regulating the expression of p-STAT3 (Ser727) and decreased the expression of upstream genes of STAT3. To further investigate the effect ropivacaine on mitoSTAT3 expression, the p-STAT3 (Ser727) expression was detected in the mitochondrial fraction and cytoplasmic fraction, which was used to determine that the mitoSTAT3 translocation in PC12 cells Results showed that mitoSTAT3 translocation was inhibited by ropivacaine. We also confirmed this by immunofluorescence staining, the co-localization of p-STAT3 (Ser727) in the mitochondria was significantly reduced after ropivacaine treatment. The anti-apoptotic effect of mitoSTAT3 has been demonstrated in many studies. Li et al. reported that the STAT3 activation is key for the ischemic postconditioning, and the increased of mitoSTAT3 can protect the cardiomyocytes against mitochondrial dysfunction (Li H et al., 2016). Zhang et al. reported Serine 727 (Ser727) phosphorylation of STAT3 plays a role in the regulation of mitochondrial respiration(Zhang G et al., 2018). In addition, mitoSTAT3 translocation can improve the oxidative phosphorylation and inhibit ROS generation during reperfusion. As we know, STAT3 activation depends on the phosphorylation of its hydrophobic domain, our results showed that ropivacaine could bind to the hydrophobic domain of STAT3, and this phosphorylation was inhibited, which confirms above findings. At last, we compared the levels of apoptosis and p-STAT3 (Ser727) expression in the spinal cord with the treatment of different concentrations of ropivacaine. The results showed that ropivacaine increased the apoptosis of the spinal cord in a dose-dependent manner, and the expression of p-STAT3 (Ser727) decreased significantly after ropivacaine treatment. This indicates that there was a negative relationship between p-STAT3 expression and apoptosis in the spinal cord. The above findings indicate ropivacaine can induce the neurotoxicity by promoting apoptosis via down-regulating STAT3 phosphorylation.

Conclusion

In conclusion, ropivacaine decreased cell viability and reduced protrusions of PC12 cells to induce neurotoxicity. Furthermore, ropivacaine arrested PC12 cells in the G0/G1 cycle phase, and promoted cell apoptosis through the mitochondrial pathway. Moreover, it also induces the Cellular Oxidative Stress and mitochondrial dysfunction in PC12 cells. These effects may be related to the inhibition of STAT3 activation and mitoSTAT3 translocation. These findings suggest STAT3 may serve as a target in the prevention a treatment of ropivacaine induced neurotoxicity

Declarations

Acknowledgements

The Innovative Research Program for Graduates of Hubei University of medicine (NO. YC2020029)

Conflicts of interest

The authors declare no conflicts of interest regarding this study and publication.

Author Contributions

LHY and DXD designed studies, ZL and ZZ undertook the cell experiments and the construction of animal experiments, CHX and WQS undertook the molecular biology testing, ZL, HJF undertook the molecular docking. ZL, ZFY, LCG analyzed data and wrote the draft of manuscript.

Ethical Approval

All procedures performed in studies involving animals were in accordance with the ethical standards of the institution or practice at the Animal Ethics Committee of the Hubei University of Medicine. (permit number: 2018DW003)

Data Availability Statement

Data that support study findings are available with the corresponding author upon reasonable request.

References

1. A B, S F, G L, D B (2017), Transient neurologic symptoms (TNS) after intrathecal injection of ropivacaine through a dural tap during an attempted epidural for labour pain relief. Anaesthesia, critical care & pain medicine 36:325-326.
2. Aps J, Badr N (2020), Narrative review: the evidence for neurotoxicity of dental local anesthetics. Journal of dental anesthesia and pain medicine 20:63-72.
3. Byram SC, Bialek SE, Husak VA, Balcarcel D, Park J, Dang J, Foecking EM (2020), Distinct neurotoxic effects of select local anesthetics on facial nerve injury and recovery. Restorative neurology and neuroscience 38:173-183.
4. Cai XY, Xia Y, Yang SH, Liu XZ, Shao ZW, Liu YL, Yang W, Xiong LM (2015), Ropivacaine- and bupivacaine-induced death of rabbit annulus fibrosus cells in vitro: involvement of the mitochondrial apoptotic pathway. Osteoarthritis and cartilage 23:1763-1775.
5. Chen Y, Yan L, Zhang Y, Yang X (2019), The role of DRP1 in ropivacaine-induced mitochondrial dysfunction and neurotoxicity. Artificial cells, nanomedicine, and biotechnology 47:1788-1796.
6. CM C, GR T, LG M, A P, LA N, M F-M, AL dO, S A, et al. (2012), Local neurotoxicity and myotoxicity evaluation of cyclodextrin complexes of bupivacaine and ropivacaine. Anesthesia and analgesia

115:1234-1241.

7. Cui P, Wei F, Hou J, Su Y, Wang J, Wang S (2020), STAT3 inhibition induced temozolomide-resistant glioblastoma apoptosis via triggering mitochondrial STAT3 translocation and respiratory chain dysfunction. Cellular signalling 71:109598.
8. El-Deiry WS (2016), p21(WAF1) Mediates Cell-Cycle Inhibition, Relevant to Cancer Suppression and Therapy. Cancer research 76:5189-5191.
9. Fathi N, Rashidi G, Khodadadi A, Shahi S, Sharifi S (2018), STAT3 and apoptosis challenges in cancer. International journal of biological macromolecules 117:993-1001.
10. Flanagan SE, Haapaniemi E, Russell MA, Caswell R, Allen HL, De Franco E, McDonald TJ, Rajala H, et al. (2014), Activating germline mutations in STAT3 cause early-onset multi-organ autoimmune disease. Nature genetics 46:812-814.
11. Guanizo AC, Fernando CD, Garama DJ, Gough DJ (2018), STAT3: a multifaceted oncoprotein. Growth factors (Chur, Switzerland) 36:1-14.
12. Guryay D, Karaege G, Katircioglu K, Ozkalkanli M, Ozgurbuz U, Savaci S (2008), The effects of an epidural infusion of ropivacaine versus saline on sensory block after spinal anesthesia. Regional anesthesia and pain medicine 33:217-221.
13. Heusch G, Musiolik J, Gedik N, Skyschally A (2011), Mitochondrial STAT3 activation and cardioprotection by ischemic postconditioning in pigs with regional myocardial ischemia/reperfusion. Circulation research 109:1302-1308.
14. Hillmer EJ, Zhang H, Li HS, Watowich SS (2016), STAT3 signaling in immunity. Cytokine & growth factor reviews 31:1-15.
15. Li H, Yao W, Liu Z, Xu A, Huang Y, Ma XL, Irwin MG, Xia Z (2016), Hyperglycemia Abrogates Ischemic Postconditioning Cardioprotection by Impairing AdipoR1/Caveolin-3/STAT3 Signaling in Diabetic Rats. Diabetes 65:942-955.
16. Lim S, Kaldis P (2013), Cdks, cyclins and CKIs: roles beyond cell cycle regulation. Development (Cambridge, England) 140:3079-3093.
17. Lirk P, Haller I, Colvin HP, Lang L, Tomaselli B, Klimaschewski L, Gerner P (2008), In vitro, inhibition of mitogen-activated protein kinase pathways protects against bupivacaine- and ropivacaine-induced neurotoxicity. Anesthesia and analgesia 106:1456-1464, table of contents.
18. Martin-Flores M (2019), Epidural and Spinal Anesthesia. The Veterinary clinics of North America Small animal practice 49:1095-1108.
19. S C, S S (2018), The role of local anaesthetic techniques in ERAS protocols for thoracic surgery. Journal of thoracic disease 10:1998-2004.
20. S W, Q L, Z W, X P (2019), Ropivacaine induces neurotoxicity by activating MAPK/p38 signal to upregulate Fas expression in neurogliocyte. Neuroscience letters 706:7-11.
21. Schade AE, Oser MG, Nicholson HE, DeCaprio JA (2019), Cyclin D-CDK4 relieves cooperative repression of proliferation and cell cycle gene expression by DREAM and RB. Oncogene 38:4962-

4976.

22. Sgrignani J, Garofalo M, Matkovic M, Merulla J, Catapano CV, Cavalli A (2018), Structural Biology of STAT3 and Its Implications for Anticancer Therapies Development. Int J Mol Sci 19.
23. Srivastava J, DiGiovanni J (2016), Non-canonical Stat3 signaling in cancer. Molecular carcinogenesis 55:1889-1898.
24. Steward-Tharp SM, Laurence A, Kanno Y, Kotlyar A, Villarino AV, Sciume G, Kuchen S, Resch W, et al. (2014), A mouse model of HIES reveals pro- and anti-inflammatory functions of STAT3. Blood 123:2978-2987.
25. Szczepanek K, Chen Q, Derecka M, Salloum FN, Zhang Q, Szelag M, Cichy J, Kukreja RC, et al. (2011), Mitochondrial-targeted Signal transducer and activator of transcription 3 (STAT3) protects against ischemia-induced changes in the electron transport chain and the generation of reactive oxygen species. The Journal of biological chemistry 286:29610-29620.
26. Takenami T, Yagishita S, Asato F, Arai M, Hoka S (2002), Intrathecal lidocaine causes posterior root axonal degeneration near entry into the spinal cord in rats. Regional anesthesia and pain medicine 27:58-67.
27. Vogel TP, Milner JD, Cooper MA (2015), The Ying and Yang of STAT3 in Human Disease. Journal of clinical immunology 35:615-623.
28. W Z, BM G (2008), The toxicity of local anesthetics: the place of ropivacaine and levobupivacaine. Current opinion in anaesthesiology 21:645-650.
29. Wang S, Lin Q, Wang Z, Pan X (2019), Ropivacaine induces neurotoxicity by activating MAPK/p38 signal to upregulate Fas expression in neurogliocyte. Neurosci Lett 706:7-11.
30. Wen X, Li Y, Liu X, Sun C, Lin J, Zhang W, Wu Y, Wang X (2019), Roles of CaMKIIβ in the neurotoxicity induced by ropivacaine hydrochloride in dorsal root ganglion. Artificial cells, nanomedicine, and biotechnology 47:2948-2956.
31. Xu W, McArthur G (2016), Cell Cycle Regulation and Melanoma. Current oncology reports 18:34.
32. Y C, L Y, Y Z, X Y (2019), The role of DRP1 in ropivacaine-induced mitochondrial dysfunction and neurotoxicity. Artificial cells, nanomedicine, and biotechnology 47:1788-1796.
33. Y H, L W, J G, X J, F J, J Y (2016), A modified procedure for lumbar intrathecal catheterization in rats. Neurological research 38:725-732.
34. Yamashita A, Matsumoto M, Matsumoto S, Itoh M, Kawai K, Sakabe T (2003), A comparison of the neurotoxic effects on the spinal cord of tetracaine, lidocaine, bupivacaine, and ropivacaine administered intrathecally in rabbits. Anesthesia and analgesia 97:512-519, table of contents.
35. Yang R, Rincon M (2016), Mitochondrial Stat3, the Need for Design Thinking. International journal of biological sciences 12:532-544.
36. You L, Wang Z, Li H, Shou J, Jing Z, Xie J, Sui X, Pan H, et al. (2015), The role of STAT3 in autophagy. Autophagy 11:729-739.

37. Z N, J T, Y R, W F (2018), Ropivacaine impairs mitochondrial biogenesis by reducing PGC-1α. Biochemical and biophysical research communications 504:513-518.
38. Z S, H L, Q G, X X, Z Z, N W (2012), In vivo and in vitro evidence of the neurotoxic effects of ropivacaine: the role of the Akt signaling pathway. Molecular medicine reports 6:1455-1459.
39. Zeng Y, Wang R, Bian Y, Chen W, Peng L (2019), Catalpol Attenuates IL-1β Induced Matrix Catabolism, Apoptosis and Inflammation in Rat Chondrocytes and Inhibits Cartilage Degeneration. Medical science monitor : international medical journal of experimental and clinical research 25:6649-6659.
40. Zhang G, Sheng M, Wang J, Teng T, Sun Y, Yang Q, Xu Z (2018), Zinc improves mitochondrial respiratory function and prevents mitochondrial ROS generation at reperfusion by phosphorylating STAT3 at Ser(727). Journal of molecular and cellular cardiology 118:169-182.

Figures

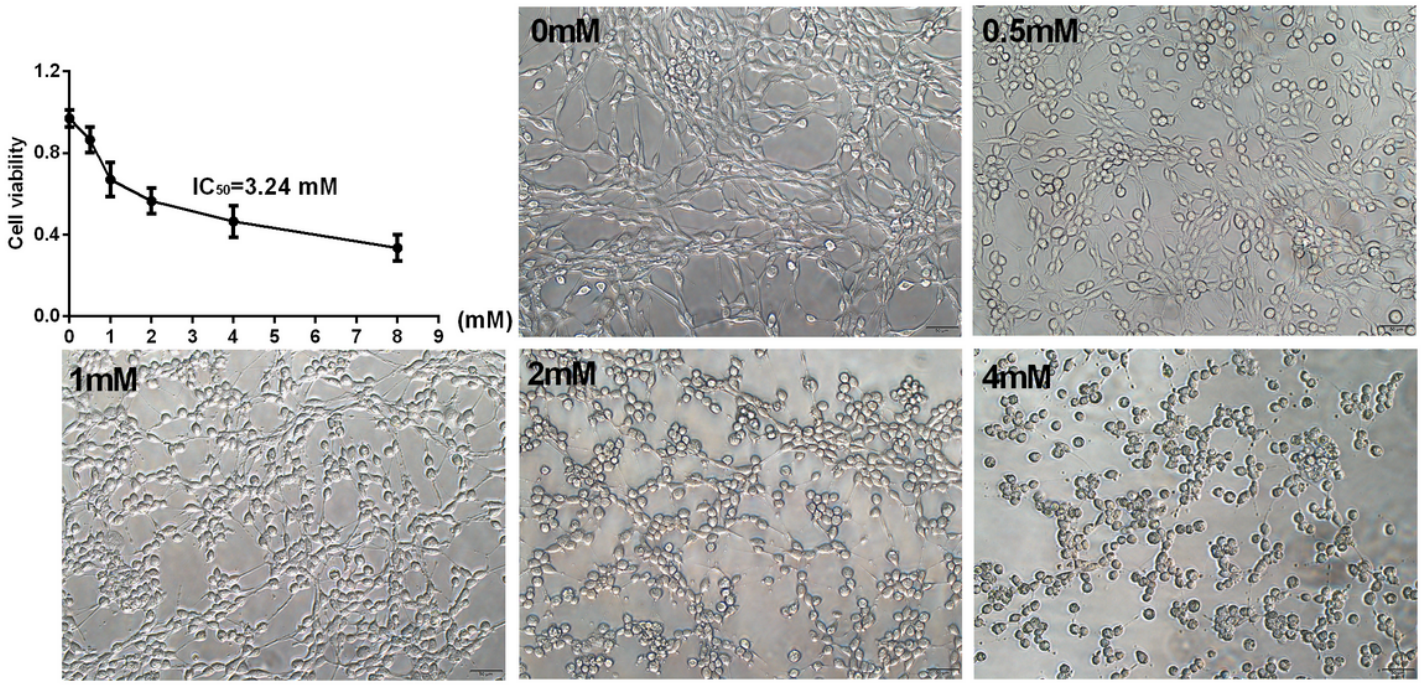

Figure 1

Ropivacaine decreased viability and reduced the protrusions of PC12 cells. (A) PC12 cells were treated with various concentrations of ropivacaine (0.5 mM, 1mM, 2 mM, 4 mM, 8mM) for 24 h, the cell viability was detected by CCK-8. (B) PC12 cells were treated as above, the cell morphology was observed by microscope (x200). The results are presented as the mean ± SD (n = 3), where * p < 0 .05, ** p < 0 .01 compared with the control.

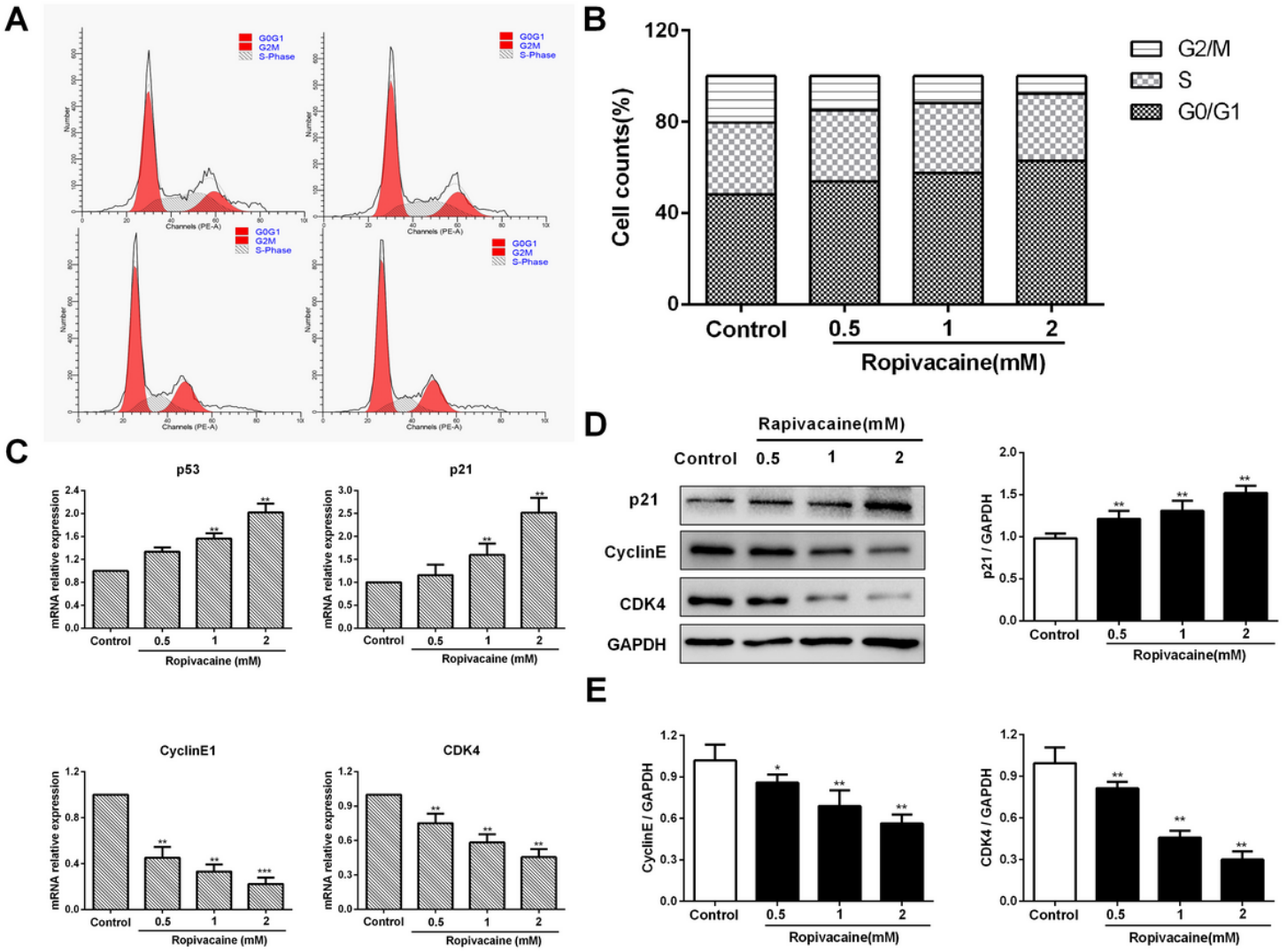

Figure 2

Ropivacaine arrested PC12 cell cycle in the G0 / G1 phase via up-regulating p21 expression and inhibiting CDK4, CyclinE1. (A) PC12 cells were treated with different concentration of ropivacaine, the cell cycle was detected by flow cytometry. (B) the quantification of cell cycle included G0/G1 phase, S phase and G2/M phase. (C) The mRNA expression of p53, p21, CDK4, CyclinE1 were detected by qRT-PCR. (D) The protein expression of p21, CDK4, CyclinE1 were detected by Western-blot. (E) Quantification of the gray values in graph D. The results are presented as the mean ± SD (n = 3), where * p < 0 .05, ** p < 0 .01 compared with the control.

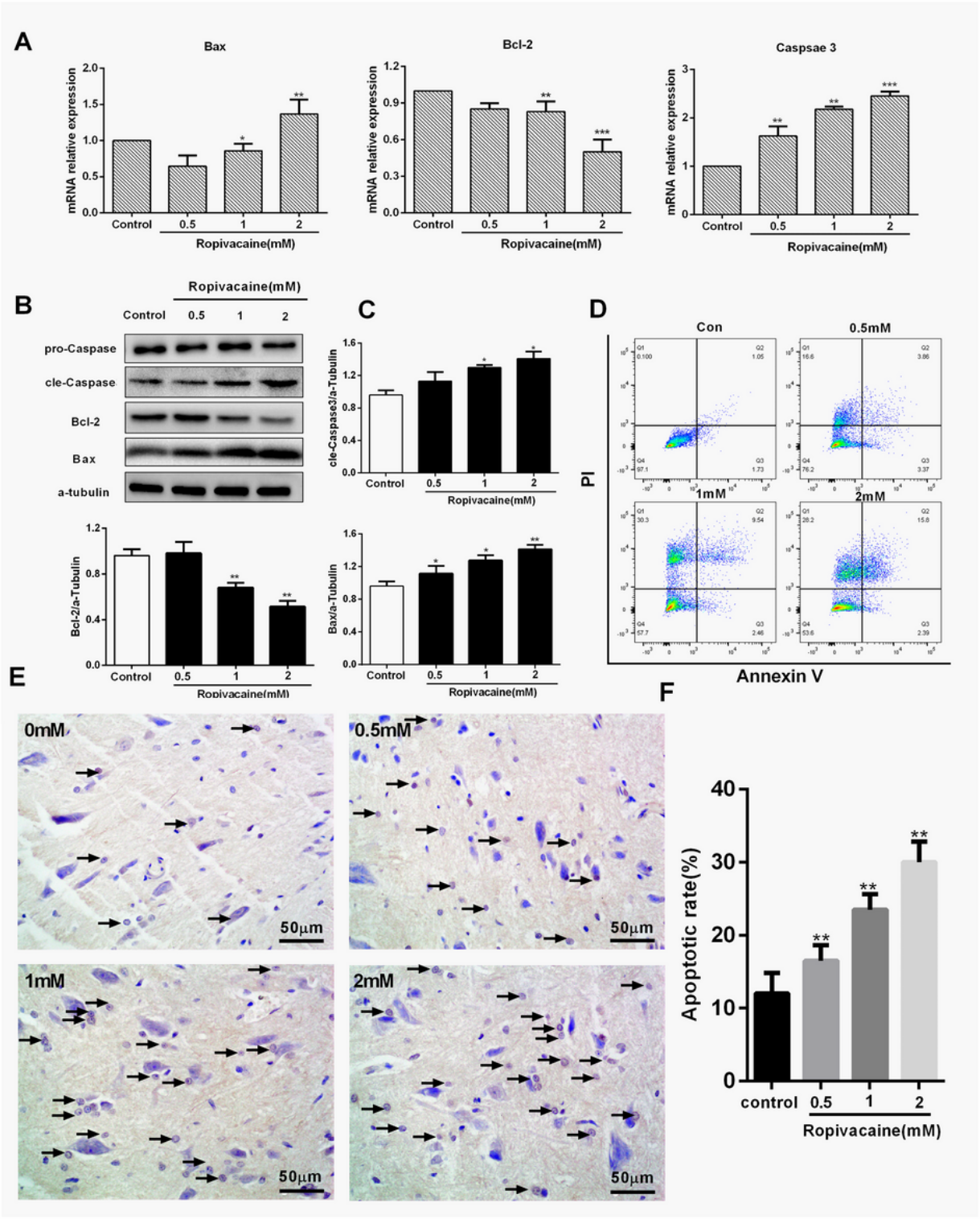

Figure 3

Ropivacaine induced apoptosis of PC12 cells and the spinal cord (A) The mRNA expression of Bax, Bcl-2 and caspase 3 in PC12 cells were detected by qRT-PCR. (B) The protein expression of Bax, Bcl-2, Caspase 3 and Cleaved-caspase-3 in PC12 cells were detected by Western-blot. (C) Quantification of the gray values in graph B. (D) The levels of apoptosis were detected by flow cytometry. (E) Rats were received the subarachnoid catheterization, and injected with different concentration of ropivacaine, the apoptosis of

spinal cord was detected by TUNNEL staining. Arrows refer to apoptotic cells. (F) The ratio of the numbers of apoptotic cells than total cells. The results are presented as the mean ± SD (n = 3), where * p < 0 .05, ** p < 0 .01, *** p < 0 .001 compared with the control.

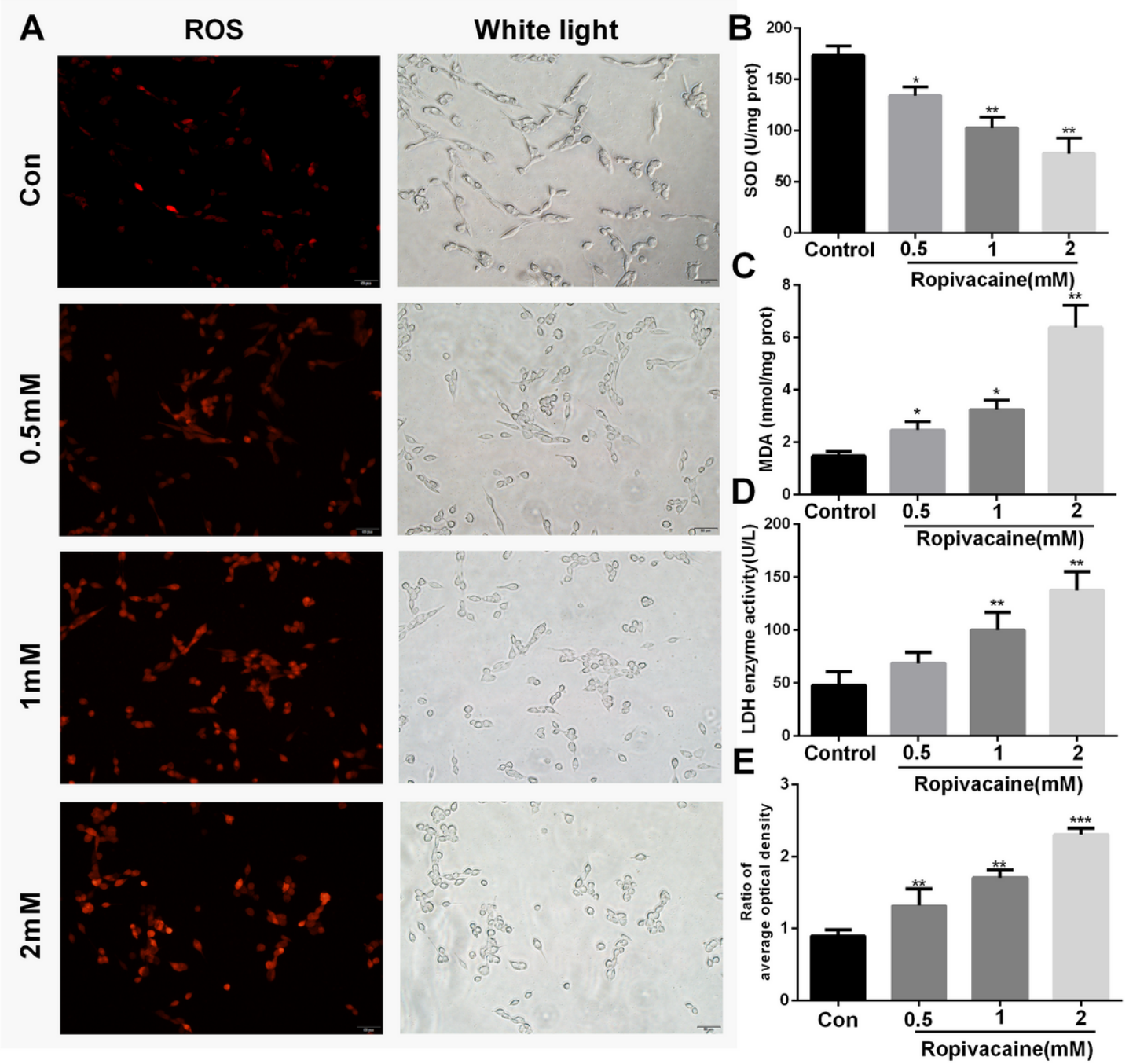

Figure 4

Ropivacaine induced oxidative stress in PC12 cells. (A) PC12 cells were treated with different concentration of ropivacaine, Intracellular ROS was determined by DHC assay. (B) (C) (D) SOD, MDA and LDH were detected by the assay kits. (E) The ratio of the average optical density in graph A. The results are presented as the mean ± SD (n = 3), where * p < 0 .05, ** p < 0 .01, *** p < 0 .001 compared with the control. (F)

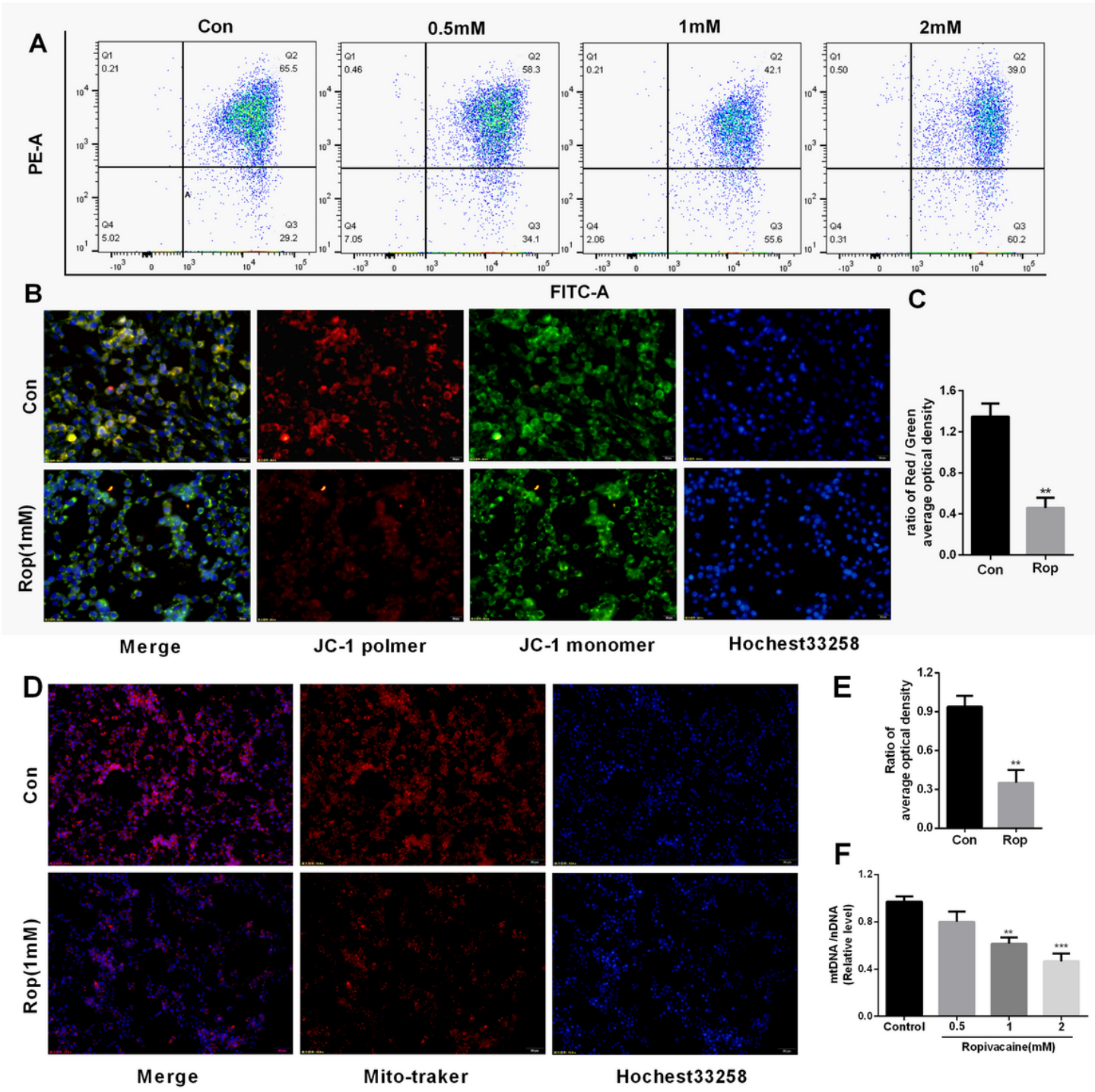

Figure 5

Ropivacaine induced PC12 cells mitochondrial dysfunction. (A) (B) PC12 were treated with different concentration of ropivacaine, mitochondrial function was detected by a JC-1 assay kit and quantified by the flow cytometry and observed in fluorescence microscope. (C) The ratio of Red / Green average optical density in graph B. (D) PC12 cells mitochondrial was labeled by the Mito-Tracker Red CMXRos and observed in fluorescence microscope. (E) The ratio of mtDNA to nDNA (mtDNA / nDNA) was measured by

qRT-RCR. The results are presented as the mean ± SD (n = 3), where ** p < 0 .01, *** p < 0 .001 compared with the control.

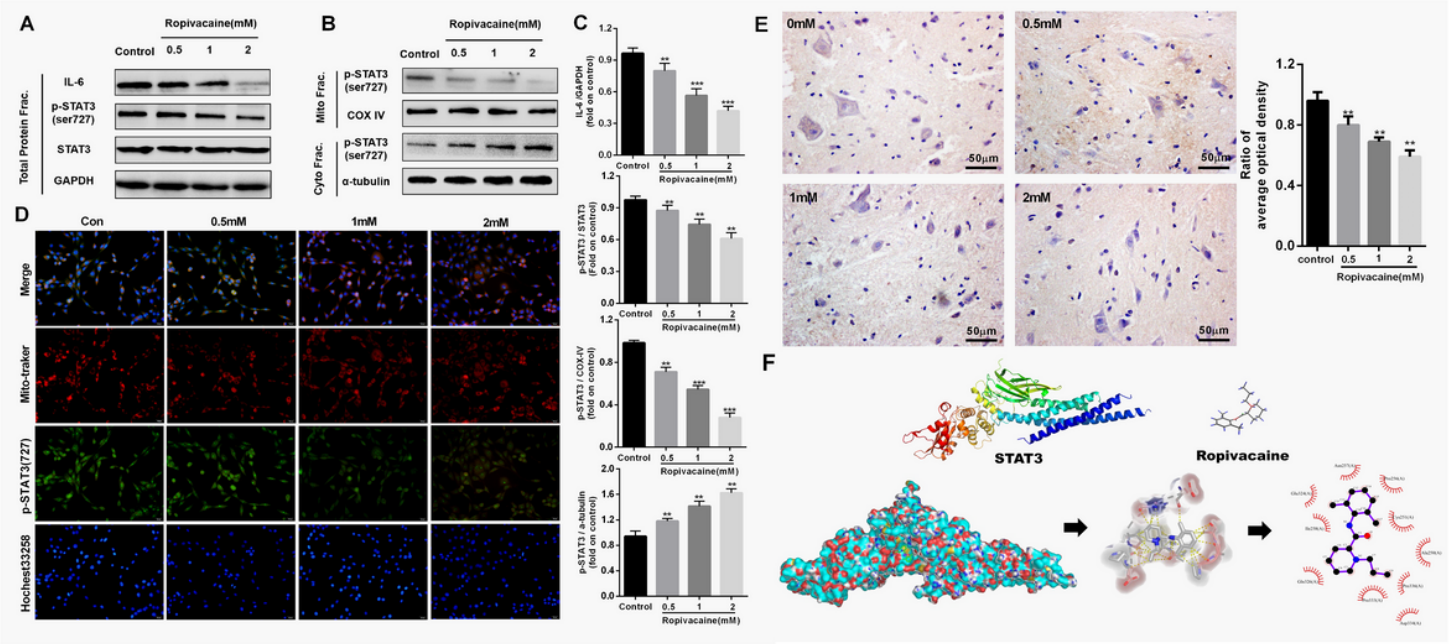

Figure 6

The effects of ropivacaine on the STAT3 signaling pathway. (A) PC12 cells were treated with different concentration of ropivacaine. The protein expression of IL-6, STAT3, p-STAT3 (Ser727) and GAPDH in total protein were detected by Western-blot. (B) The protein expression of p-STAT3 (Ser727) in mitochondrial and cytoplasmic were detected by Western-blot. (C) Quantification of the gray values in graph A and B. (D) Effect of ropivacaine on the colocalization of mitochondria (red) and STAT3(green) were detected by fluorescence microscope, and were represented as the overlapping fluorescence for the red and green channels, where the combined pixels appeared yellow. (E) Rats were received the subarachnoid catheterization, and injected with different concentration of ropivacaine, the expression of p-STAT3 (Ser727) in the spinal cord was measured by Immunohistochemistry. (F) Computational modeling of ropivacaine binding to the STAT3.The results are presented as the mean ± SD (n = 3), where ** p < 0 .01, *** p < 0 .001 compared with the control.